

Resonant Tunneling through Electronic Trapping States in Thin MgO Magnetic Junctions

J. M. Teixeira,* J. Ventura, J. P. Araujo, and J. B. Sousa

IFIMUP and IN-Institute of Nanoscience and Nanotechnology, and Departamento de Física, Faculdade de Ciências, Universidade do Porto, Rua do Campo Alegre, 687, 4169-007 Porto, Portugal

P. Wisniowski

*Department of Electronics, AGH University of Science and Technology, 30-059 Krakow, Poland
INESC-MN and IN-Institute of Nanoscience and Nanotechnology, Rua Alves Redol, 9-1, 1000-029 Lisbon, Portugal*

S. Cardoso and P. P. Freitas

*INESC-MN and IN-Institute of Nanoscience and Nanotechnology, Rua Alves Redol, 9-1, 1000-029 Lisbon, Portugal
(Received 5 November 2010; published 10 May 2011)*

We report an inelastic electron tunneling spectroscopy study on MgO magnetic junctions with thin barriers (0.85–1.35 nm). Inelastic electron tunneling spectroscopy reveals resonant electronic trapping within the barrier for voltages $V > 0.15$ V. These trapping features are associated with defects in the barrier crystalline structure, as confirmed by high-resolution transmission electron microscopy. Such defects are responsible for resonant tunneling due to energy levels that are formed in the barrier. A model was applied to determine the average location and energy level of the traps, indicating that they are mostly located in the middle of the MgO barrier, in accordance with the high-resolution transmission electron microscopy data and trap-assisted tunneling conductance theory. Evidence of the influence of trapping on the voltage dependence of tunnel magnetoresistance is shown.

DOI: [10.1103/PhysRevLett.106.196601](https://doi.org/10.1103/PhysRevLett.106.196601)

PACS numbers: 85.30.Mn, 72.10.Fk, 73.40.Gk, 85.35.-p

Magnetic tunnel junctions (MTJs) with MgO barriers are a subject of great research interest due to their huge number of applications, such as forefront spin-transfer-torque magnetic random access memories, read heads, and novel microwave devices [1–3]. This results from the theoretically predicted [4] and experimentally verified giant tunnel magnetoresistance (TMR) effect [5,6]. However, the reported TMR values are always considerably lower than those predicted, particularly in the ultrathin barrier limit. Also, fittings to current-voltage (I - V) curves indicate barrier heights of ~ 0.5 – 1.5 eV [5,6], well below bulk values and those obtained from scanning tunneling spectroscopy [7]. These discrepancies have been attributed to the presence of vacancies and other structural defects within the barrier [5,6,8–17], plus disorder and oxidation at the ferromagnetic- (FM-)barrier interface [18,19], all having a detrimental impact on TMR. The drop of TMR with bias voltage (V) [5,20,21] is also a matter of great importance, not only because of its fundamental physical interest but also because of its impact on applications. To explain such a decrease, several mechanisms have been proposed, including excitation of magnons at the FM-barrier interface [20], the energy dependence of the spin-polarized density of states [22,23], and incoherent tunneling due to scattering at impurities or defects in the barrier [12–14].

Particularly relevant to unravel tunneling mechanisms in MTJs is inelastic electron tunneling spectroscopy (IETS), obtained by taking the second derivative of the I - V characteristic of MTJs. With this powerful method, one is

able to detect various sorts of elementary excitations in the barrier, FM electrodes, or interfaces [21,24–26]. It can also be used to investigate impurity scattering and characterize the structure of the FM-barrier interfaces and the band structure of the electrodes [24,27,28]. IETS is thus a useful tool to investigate transport processes and tunneling mechanisms in MTJs, shedding light on the bias dependence of tunnel conductance ($G \equiv dI/dV$) and TMR. IETS is also an important technique in the characterization of semiconductor devices and molecular junctions [29,30].

In this work, we study the IETS spectra of sputtered pinhole-free CoFeB/MgO/CoFeB MTJs with thin barriers ($t_b \sim 1$ nm) and exhibiting room temperature (RT) TMR values above 100% [31], thus allowing us to identify tunnel conduction related features. The IETS spectra is analyzed for both magnetic states [parallel (P) and antiparallel (AP)] at low ($T = 20$ K) and RT, in a set of MTJs with varying MgO thickness (0.85–1.35 nm). At low bias ($V \leq 0.15$ V), the differences between the P and AP IETS spectra are assigned to the excitation of magnons [20,21,24,25], while for higher bias we observe the dominance of electronic trapping processes occurring in the MgO barrier. Two kinds of traps will be identified: those contributing to trap-assisted tunneling and those contributing to charge trapping. From the polarity dependence of the IETS spectra, we determined the average location and energy levels of the traps in the MgO. These trapping features are associated with defects in the MgO barrier, as confirmed by high-resolution transmission electron microscopy

(HRTEM). Finally, we show that such trapping mechanisms have an important contribution to TMR(V).

The set of MTJs with areas ranging between 1×3 and $3 \times 6 \mu\text{m}^2$ was deposited in a magnetron sputtering system (Nordiko 2000) with a base pressure of 7×10^{-9} Torr in dc and rf (CoFe and MgO) modes. The complete structure was glass/Ta 5 nm/Ru 18 nm/Ta 3 nm/Mn₅₄Pt₄₆ 20 nm/Co₈₂Fe₁₈ 2.2 nm/Ru 0.9 nm/CoFeB 3 nm/MgO(t_b)/CoFeB 3 nm/Ru 5 nm/Ta 5 nm, where CoFeB stands for (Co₅₂Fe₄₈)₇₅B₂₅ and $t_b = 0.85, 1.05, 1.15,$ and 1.35 nm. A detailed description of fabrication and measurement conditions can be found in Refs. [32,33]. Our IETS curves were obtained by numerically differentiating the I - V experimental data, within a voltage range that depends on t_b . Positive (negative) bias indicates electron flow from the bottom (top) to the top (bottom) electrodes. Figure 1(a) shows an example of a HRTEM image of these stacks after annealing, where an overall good crystalline texture is seen.

The first derivative of the conductance (dG/dV) of MTJs with $t_b = 1.05$ and 1.35 nm is shown in Fig. 2 for positive [(a) and (c)] and negative [(b) and (d)] bias voltages and for the P and AP states at $T = 20$ K. To compare samples with different conductances, dG/dV was normalized by the zero bias conductance in each case [24]. Large peaks at low bias ($|V| \leq 0.15$ V) in the IETS spectrum for the AP state are seen in all samples, which differs considerably from the P spectra. These peaks with maxima between ± 0.05 and ± 0.1 V are attributed to magnon excitation, since they strongly depend on the magnetic configuration [20,21,24,25]. The much larger dG/dV signal for AP state is a consequence of the larger contribution of spin wave excitation, which is in agreement with the T dependence of both G and TMR at low bias [31]. Despite the large contribution arising from magnon excitation, we should mention that the first and largest peak observed in the AP state of the IETS spectra extends up to 0.3 V, well beyond the magnon linear response regime in the FM

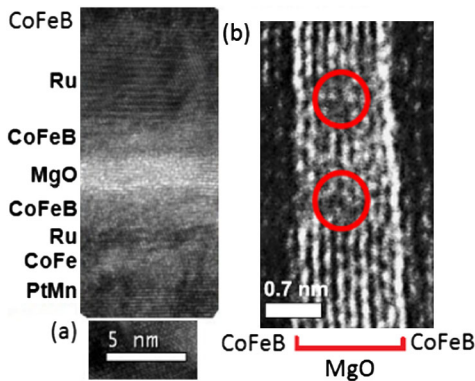


FIG. 1 (color online). (a) HRTEM picture of the MTJ stacks after annealing. (b) Enlarged image from the CoFeB/MgO/CoFeB layers only. Circles indicate defects or disorder in the MgO barrier.

electrode. In fact, there is a small valley following the first (largest) peak of the AP IETS spectra that could correspond (partly) to a barrier state but is largely masked by magnon contribution at low bias. Also, the valley of the P IETS spectra in the 0–0.3 V range is related with a minimum of the $G_P(V)$ curve (not shown), occurring at ~ 0.3 V and associated with the electronic band structure of the CoFeB electrodes [34]. In fact, the top of majority-spin Δ_2^{\uparrow} and Δ_5 bands in Fe lie ~ 0.2 V above the Fermi level (E_F), while for Co the top of minority-spin Δ_2 band lies ~ 0.3 V above E_F [1]. When the energy of the tunneling electrons overcomes the top of these bands, the conduction channel associated with this state disappears and $G_P(V)$ decreases.

For higher voltages and in both magnetic states, the IETS spectra clearly show anomalies which consist of both peaks and valleys. This kind of anomalies is a characteristic of elastic electronic trapping processes occurring in an insulating barrier or at a metallic-insulator interface and is distinguishable from other (inelastic) tunneling mechanisms (e.g., magnons and phonons) which appear only as peaks [29]. In fact, and although the primary features in an IETS spectrum are due to inelastic tunneling, it also displays significant contributions from elastic processes. As clearly seen in Fig. 2, such IETS features are characterized either by peaks followed by valleys [e.g., the oscillation labeled by circle 1 in Fig. 2(a)], corresponding to trap-assisted tunneling [Fig. 3(a)], or by valleys followed by peaks [e.g., the oscillation labeled by circle 2' in Fig. 2(b)], associated with charge trapping [see Fig. 3(a)]. In fact, trap-assisted conduction (charge trapping) leads to an increase (decrease) in the slope of the I - V curve over a small voltage range [29]. Moreover, the shape of the trapping features is very similar for both positive and negative bias regions in each IETS spectra, indicating that they originate from the same traps. The generally different IETS trap intensity between positive and negative bias

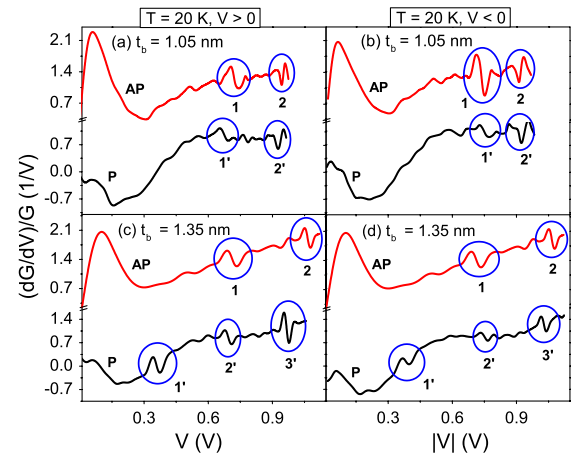


FIG. 2 (color online). IETS spectra for $V > 0$ [(a) and (c)] and $V < 0$ [(b) and (d)] in the P and AP states at 20 K. The spectra were obtained in the MTJs with $t_b = 1.05$ [(a) and (b)] and 1.35 nm [(c) and (d)].

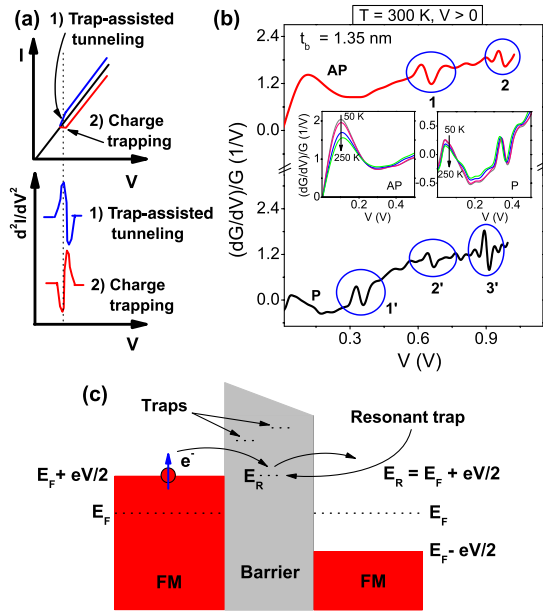


FIG. 3 (color online). (a) Schematic illustrating the two kind of traps revealed by the IETS spectra. (b) Selected IETS spectra at RT for $V > 0$ and the P and AP states ($t_b = 1.35$ nm). Insets show IETS spectra at several T ($= 50, 100, 200,$ and 250 K). (c) Schematic diagram of a tunnel barrier bounded by the two FM electrodes, with a voltage bias such that the trap energy level coincides with the Fermi level (E_F) of the left electrode, allowing, e.g., trap-assisted tunneling.

regions of each sample (Fig. 2) can be explained by the usual asymmetry of the tunnel barrier [29].

The electronic properties of oxide materials are strongly affected by the presence of defects (vacancies, dislocations, and step edges) in their crystal structure [35,36]. Besides locally perturbing the lattice, these defects can also induce discrete electronic states in the oxide band gap that can trap or assist tunneling electrons, as recently shown for the case of isolated vacancies in thin MgO barriers [12]. In fact, in MgO electrons can be trapped inside dislocations, oxygen vacancies, or grain boundaries [35,36]. Oxygen vacancies also lead to a substantial reduction of TMR in MgO junctions due to incoherent elastic scattering of tunneling electrons [12–14,17], and a recent study showed the influence of misfit dislocations on the TMR of MgO-based epitaxial MTJs [16].

When E_F of one of the electrodes is resonant with the energy level of the trap (V_{trap}), a trapping process will start to take place [Fig. 3(c)]. The width and height of the IETS trap related feature correspond to the energy and spatial distribution of these traps, respectively [37]. Since this process is elastic, one should expect a weak dependence on temperature, in contrast with the stronger dependence of an inelastic tunneling event [29]. This is experimentally confirmed in Fig. 3(b), where the IETS features associated with trapping do not change significantly with T . In contrast, note that the peaks at lower voltages ($|V| \leq 0.15$ V) related with inelastic magnon interactions become

considerably smoother with the increase of T [inset in Fig. 3(b)]. The effect is higher for the AP IETS spectra than for the P state, confirming that magnon excitations play an important role in this low bias range.

Based on a simple model [29], one can estimate both the average physical location (t_{trap}) and energy level (V_{trap}) of the traps, given by

$$V_{\text{trap}} = \frac{V_{\text{pos}} V_{\text{neg}}}{V_{\text{pos}} + V_{\text{neg}}}; \quad t_{\text{trap}} = \frac{t_b V_{\text{pos}}}{V_{\text{pos}} + V_{\text{neg}}}, \quad (1)$$

where V_{pos} and V_{neg} are the voltages at which the trap feature occurs in positive and negative biased IETS spectra. The t_{trap}/t_b ratios of the studied MTJs are between 0.47 and 0.53, indicating that the centroid of the probed traps is located approximately in the middle of the barrier. This is experimentally confirmed by HRTEM images [Fig. 1(b)], showing the presence of defect regions distributed roughly in the middle of the MgO barrier. To further deepen our study, one can use the theoretically predicted trap-assisted tunneling conductance (G_{TAT}) via one localized state [38]:

$$G_{\text{TAT}}(E \mapsto E') = \frac{e^2}{2\pi\hbar} \frac{4\Gamma_L\Gamma_R}{(E - E_{\text{trap}})^2 + \Gamma^2} \delta(E - E'), \quad (2)$$

where E and E' are the initial and final electron energy, respectively, via a localized state with energy E_{trap} , and $\Gamma_{L,R} \propto \exp(-2\alpha t_{L,R})$. The δ function means energy conservation, $\Gamma = \Gamma_L + \Gamma_R$, α^{-1} is the localization length, and $t_{L(R)}$ is the distance from the trap to the left (right) electrode. Thus, G_{TAT} reaches its maximum ($e^2/2\pi\hbar$) when $E = E_{\text{trap}} = E'$ and $\Gamma_L = \Gamma_R$ (i.e., $t_L = t_R = t_b/2$). The maximum transmission probability for elastic tunneling through one localized state thus occurs when such a trap is localized in the middle of the barrier, in excellent agreement with our experimental findings.

Also, we found trapping states with energies between 0.15 and 0.53 eV above E_F of the FM electrodes. Moreover, we observe that the trapping level 1' of the thicker MTJ [Figs. 2(c) and 2(d)] is not observable in the AP state. Although a masking effect due to the higher intensity of the IETS spectra in the AP state cannot be discarded, we should also consider the possibility of resonant tunneling through spin-polarized defects. In fact, a recent study [39] provided evidence of the appearance of magnetic moments in MgO that arise from the spin polarization of $2p$ orbitals of oxygen atoms nearest to Mg vacancies. As theoretically discussed in Ref. [10], such spin-polarized barrier states can have important consequences on the magnetotransport of MTJs and lead to both a TMR enhancement and reduction depending on the magnetic coupling between the electrodes. Furthermore, it was shown that the impact of spin-polarized barrier states on the TMR value becomes more evident as one moves away from the barrier-electrodes interfaces and into the center of the barrier.

One reason can be addressed to explain the intense trap features observed in the IETS spectra of the studied MTJs

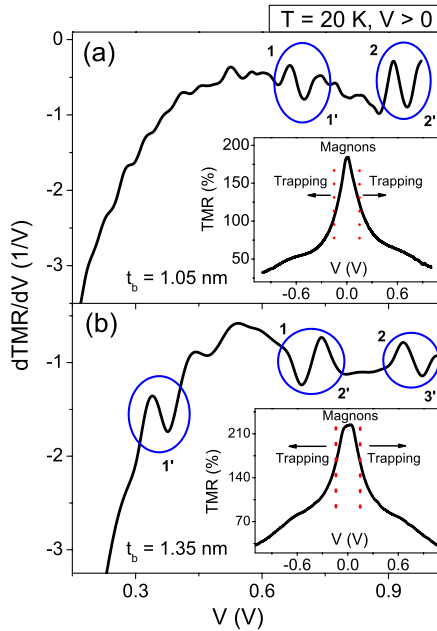


FIG. 4 (color online). Derivative of $\text{TMR}(V)$ at 20 K for $V > 0$ and for MTJs with (a) $t_b = 1.05$ and (b) 1.35 nm. The insets show the $\text{TMR}(V)$ behavior.

at elevated bias voltages. It is known that starting with a good MgO (001) texture before annealing leads to a crystallized barrier with less defects [1]. However, our samples have thin barriers belonging to the critical t_b range (1.0–1.6 nm) where the MgO deposited on the amorphous CoFeB layer can also be amorphous before annealing [40] so that the presence of defects is expected.

Finally, the influence of the trapping mechanisms on the $\text{TMR}(V)$ behavior ($\text{TMR} = G_P/G_{AP} - 1$) is illustrated in Fig. 4. Clearly, the decrease of $\text{TMR}(V)$ at higher bias voltages (see the inset in Fig. 4) has an important contribution from electronic trapping occurring in the MgO band gap due to the presence of defects. In fact, the derivative of TMR ($d\text{TMR}/dV$) shows the same type of oscillations at the same bias voltages as those observed in the IETS. At low bias (≤ 0.15 V), TMR decreases faster due to inelastic magnon excitations.

In summary, IETS on thin pinhole-free CoFeB/MgO/CoFeB MTJs has shown that electronic trapping mechanisms occurring in MgO have an important contribution to the bias dependence of their transport properties at $V > 0.15$ V, while spin wave excitation explains it at low bias. The trap locations and energy levels were estimated, revealing that most traps are located in the middle of the MgO for all the studied MTJs. This was further confirmed by HRTEM pictures.

This work was supported by Grants No. FEDERPOCTI/0155 and No. NANO/NMED-SD/0140/2007. Funding from FCT through IN is acknowledged. J. M. T. is thankful

for an FCT Grant (No. SFRH/BPD/72329/2010). P. W. and J. V. acknowledge financial support of STT NN 515544538 and FSE/POPH, respectively.

*jmteixeira@fc.up.pt

- [1] S. Yuasa *et al.*, *J. Phys. D* **40**, R337 (2007).
- [2] D. Houssameddine *et al.*, *Phys. Rev. Lett.* **102**, 257202 (2009).
- [3] Y.-T. Cui *et al.*, *Phys. Rev. Lett.* **104**, 097201 (2010).
- [4] X.-G. Zhang and W.H. Butler, *Phys. Rev. B* **70**, 172407 (2004).
- [5] S. Yuasa *et al.*, *Nature Mater.* **3**, 868 (2004).
- [6] S. S. P. Parkin *et al.*, *Nature Mater.* **3**, 862 (2004).
- [7] S. Schintke *et al.*, *Phys. Rev. Lett.* **87**, 276801 (2001).
- [8] A. M. Bratkovsky, *Phys. Rev. B* **56**, 2344 (1997).
- [9] J. Zhang *et al.*, *J. Appl. Phys.* **83**, 6512 (1998).
- [10] R. R. Jansen and J. C. Lodder, *Phys. Rev. B* **61**, 5860 (2000).
- [11] R. R. Jansen and J. S. Moodera, *Phys. Rev. B* **61**, 9047 (2000).
- [12] P. G. Mather, J. C. Read, and R. A. Buhrman, *Phys. Rev. B* **73**, 205412 (2006).
- [13] J. P. Velev *et al.*, *Appl. Phys. Lett.* **90**, 072502 (2007).
- [14] G. X. Miao *et al.*, *Phys. Rev. Lett.* **100**, 246803 (2008).
- [15] Y. Lu *et al.*, *Phys. Rev. Lett.* **102**, 176801 (2009).
- [16] F. Bonell *et al.*, *Phys. Rev. B* **82**, 092405 (2010).
- [17] Y. Ke, K. Xia, and H. Guo, *Phys. Rev. Lett.* **105**, 236801 (2010).
- [18] X.-G. Zhang, W. H. Butler, and A. Bandyopadhyay, *Phys. Rev. B* **68**, 092402 (2003).
- [19] Y. Ke, K. Xia, and H. Guo, *Phys. Rev. Lett.* **100**, 166805 (2008).
- [20] S. Zhang *et al.*, *Phys. Rev. Lett.* **79**, 3744 (1997).
- [21] J. S. Moodera, J. Nowak, and R. J. M. van de Veerdonk, *Phys. Rev. Lett.* **80**, 2941 (1998).
- [22] P. LeClair *et al.*, *Phys. Rev. Lett.* **88**, 107201 (2002).
- [23] C. Heiliger *et al.*, *Phys. Rev. B* **73**, 214441 (2006).
- [24] S. Nishioka *et al.*, *Appl. Phys. Lett.* **93**, 122511 (2008).
- [25] V. Drewello *et al.*, *Phys. Rev. B* **79**, 174417 (2009).
- [26] A. A. Khan *et al.*, *J. Appl. Phys.* **105**, 083723 (2009).
- [27] D. Ebke *et al.*, *Appl. Phys. Lett.* **95**, 232510 (2009).
- [28] G. X. Du *et al.*, *Phys. Rev. B* **81**, 064438 (2010).
- [29] J. W. Reiner *et al.*, *Adv. Mater.* **22**, 2962 (2010).
- [30] W. Wang *et al.*, *Nano Lett.* **8**, 478 (2008).
- [31] J. M. Teixeira *et al.*, *Appl. Phys. Lett.* **96**, 262506 (2010).
- [32] J. M. Teixeira *et al.*, *J. Appl. Phys.* **106**, 073707 (2009).
- [33] J. M. Teixeira *et al.*, *Phys. Rev. B* **81**, 134423 (2010).
- [34] S. Ikeda *et al.*, *J. Appl. Phys.* **99**, 08A907 (2006).
- [35] K. P. McKenna *et al.*, *Nature Mater.* **7**, 859 (2008).
- [36] H. M. Benia *et al.*, *Phys. Rev. B* **81**, 241415(R) (2010).
- [37] Z. G. Liu *et al.*, *Appl. Phys. Lett.* **97**, 172102 (2010).
- [38] Y. Xu, D. Ephron, and M. R. Beasley, *Phys. Rev. B* **52**, 2843 (1995).
- [39] C. Martinez-Boubeta *et al.*, *Phys. Rev. B* **82**, 024405 (2010).
- [40] Y. Lu *et al.*, *Appl. Phys. Lett.* **91**, 222504 (2007).